STUDY ON CALCULATION OF LAND SURFACE EVAPOTRANSPIRATION USING REMOTE SENSING

Zhiming.Zhan[a], Qiming Qin[a], Zhaodong.Feng[b] , Xin Wang[c]

[a] Institute of RS & GIS , Peking University, Beijing, 100871, China
[b] Department of Earth and Environmental Studies, Montclair State University, Upper Montclair, NJ 07043, USA
[c] the Department of Atmospheric Science, Peking University, Beijing, 100871, Chin

Commission WG VII/2

KEY WORDS: Evapotranspiration(ET), Remote sensing, NOAA/AVHRR, Western Chinese Loess Plateau, SEBS, Land surface parameters.

ABSTRACT:
Evapotranspiration (ET) plays a significant role in regional and global climates through its partitioning in hydrological cycles, and its estimation is thus of a great importance in assessing ground water and surface water resources, predicting crop yield and planning land use. For experimenting the possibility to assess the hydrological responses of ecological restoration in the Western Chinese Loess Plateau, a daily ET is comprehensively estimated by inputting NOAA/AVHRR data-derived parameters into surface energy balance system (SEBS) model. The observed data in the Western Chinese Loess Plateau are used to verify the estimates of input variables. ET estimation in this research shows that ET in the Western Chinese Loess Plateau is primarily determined by vegetation coverage, which is in turn determined by soil water availability. This study also demonstrates the remote sensing-aided surface energy balance model can be used to estimate ET in semiarid areas.

1. INTRODUCTION

Evapotranspiration (ET) plays a significant role in regional and global climates through its partitioning in hydrological cycles, and its estimation is thus of a great importance in assessing ground water and surface water resources, predicting crop yield and planning land use. The importance is even greater in the western Chinese Loess Plateau where human-induced deterioration in ecological condition has altered the path of regional hydrological cycle, further exacerbating the ecological conditions. The altered land-surface ecological and hydrological processes greatly influence the exchanges of water (vapor) and energy (heat) between land surface and atmosphere. ET is the process that performs the water and energy exchanges. In order to understand the impacts of the human-induced deterioration in ecological and hydrological conditions, ET needs to be reliably estimated for scientifically assessing the hydrological responses of ecological restoration and for practically re-planning the land uses in the western Chinese Loess Plateau.

Unfortunately, the estimation of ET with an acceptable level of accuracy has been inhibited by lack of high-resolution temporal and spatial data. However, development in satellite remote sensing technologies provides us an opportunity to obtain such high-resolution data. The Estimation of ET using remote sensing techniques involves a series of deductive processes by indexing the relevant parameters. For example, the visible channels can be used to index the surface albedo reflecting the land surface properties. The infrared channels provide an estimate of the land surface temperature from which the vapor pressure deficit can be estimated. Near infrared and thermal infrared channels can be used to calculate the vegetation index.

In this paper, we present our research results of estimating ET in the western part of the Chinese Loess Plateau (102-108^{o}E, 34-38^{o}N) (Fig.1) using satellite remote sensing data. This approach is based on a feedback relationship in which the land surface parameters (e.g., land surface temperature, albedo, emissivity, and vegetation index) obtained from NOAA/AVHRR are applied to the surface energy balance system model (SEBS) to estimate the actual evapotranspiration. The observed data from weather stations in the western Chinese Loess Plateau are used to verify the estimates of input variables. These input variables to estimate ET include net radiation, soil heat flux, sensible heat flux, latent heat flux, albedo, NDVI, emissivity, surface temperature and evaporative fraction.

2. METHODOLOGY

2.1 Basic Model

Two basic facts made satellite remote sensing technologies attractive in estimating land-surface evapotranspiration (ET). First, satellite remote sensing is solely based on electromagnetic radiation. Second, ET is an important component in outgoing long-wave radiation from the surface to the atmosphere. Thus, by inferring the non-ET components of the electromagnetic radiation, the ET can be estimated. The surface energy balance is estimated with the surface energy balance system model (SEBS):

$$R_n = \lambda E + H + G_0 + PH \quad (1)$$

where R_n is the net radiation, H the turbulent sensible heat flux, and λE the turbulent latent heat flux (λ=2.49*10^6, Wm/mm; here E is ET), G_0 soil heat flux（W/mm）, PH the energy for

photosynthesis. PH is generally very low and can thus be ignored.

2.1.1 Net radiation R_n

Surface net radiation R_n can be calculated from the incoming and outgoing radiation fluxes

$$R_n = K^{\downarrow}(1-r) + L^{\downarrow} - L^{\uparrow} \quad (2)$$

where $K^{\downarrow}$ (0.15-4 um) is the incoming short-wave radiation, *r* land surface reflection, $L^{\downarrow}$ (>4 um) the atmospheric long-wave radiation, $L^{\uparrow}$ land surface long-wave radiation.

The incoming short-wave radiation flux $K^{\downarrow}$ in Eq 2. can be derived from radiative transfer model MODTRAN by inputting several location-dependent atmospheric parameters. Specifically, $K^{\downarrow}$ can be obtained as

$$K^{\downarrow} = \tau_s K^{\downarrow}_{TOP} \quad (3)$$

where the atmospheric short-wave transmittance τ_s can be directly derived from MODTRAN. The spectrally integrated form of in-band radiation $K^{\downarrow}_{TOP}$ is obtained as

$$K^{\downarrow}_{TOP} = \frac{K^{\downarrow}_{exo}(b)\cos\theta_{sun}}{d_s^2} \quad (4)$$

where $K^{\downarrow}_{exo}(b)$ is the mean in-band solar exo-atmospheric irradiance undisturber by the atmosphere $\theta_{sun} = 0^{\circ}$, d_s the earth-sun distance, θ_{sun} represents the sun zenith angle.

The atmospheric long-wave radiation $L^{\downarrow}$ can be expressed as (Win, et al.,1999)

$$L^{\downarrow} = \varepsilon_r \sigma T^4 + c_2 N - c_3(N - N_h) \quad (5)$$

$$\varepsilon_r = 1.24\left(\frac{e_a}{T_a}\right)^{\frac{1}{7}} \quad (6)$$

ε_r is atmosphere long-wave emissivity, T_a the atmosphere temperature on the referral height，N total cloud amount，N_h low and middle cloud amounts, c2 and c3 are experiential factors，e_a the actual vapor tension for T_a（hPa）。

Land surface long-wave radiation $L^{\uparrow}$ can be expressed as

$$L^{\uparrow} = \varepsilon_s \sigma T_s^4 + (1-\varepsilon_s)L^{\downarrow} \quad (7)$$

ε_s is land surface emissivity derived from Eq 6, σ is Stefan-Boltzmann constant. T (land surface temperature) can be derived from the bright temperature of NOAA channels 4 and 5.

2.1.2 The soil heat flux G_0

The regional soil heat flux G_0 can be determined by the following equation (Choudhury and Monteith, 1988)

$$G_0 = \rho_s C_s[(T_{sfc} - T_s)]/\gamma_{sh} \quad (8)$$

where ρ_s is soil dry bulk density, C_s soil specific heat, T_{sfc} land surface temperature , T_s stand for soil temperature at a determined height, γ_{sh} represents soil heat transportation resistance. Although G_0 can not be directly derived from satellite remote sensing data, an empirical equation, $\Gamma = G_0 / R_n$, was proposed (Menenti et al.,1991; Bastiaanssen, 1995) to calculate G_0 from remote sensing data. $\Gamma_c = 0.05$ 05 is for a full vegetation canopy (Monteith 1973) and $\Gamma_s = 0.315$ is for bare soil (Kustas and Daughtry 1989). An interpolation is then performed between these two extremes by using the fractional canopy coverage f_c derived from Eq (10). The soil heat flux G_0 can thus be parameterized as

$$G_0 = R_n \cdot [\Gamma_c + (1-f_c)\cdot(\Gamma_s - \Gamma_c)] \quad (9)$$

According to Gutman (1998) , the relationship between f_c f and NDVI is found as：

$$f_c = \frac{NDVI - NDVI_{\min}}{NDVI_{\max} - NDVI_{\min}} \quad (10)$$

$NDVI_{max}$ and $NDVI_{min}$ are the maximum and minimum *NDVI* in growth seasons. We adopt the NDVI in summer to be the $NDVI_{max}$ and 0.005 to be $NDVI_{min.}$

2.1.3 Sensible Heat flux H

The sensible heat flux (H) is the component that transfers sensible energy from land surface to atmosphere. The regional distribution of H can be estimated with a bulk transfer equation expressed in following form (Monteith,1973)

$$H = \frac{\rho C_p (T_{sfc} - T_a)}{\gamma_a} \quad (11)$$

ρ C_p is the atmosphere volume heat capacity , Ta the atmosphere temperature in the referral height , T_{sfc} land surface temperature that can be estimated by the bright temperature of NOAA channels 4 and 5, γ_a is the aerodynamics resistance.

The aerodynamics resistance γ_a i n Eq 11 is obtained based on the following edqation:

$$\gamma_a = \frac{1}{ku_*}[\ln(\frac{z-d_0}{Z_{0m}}) + kB^{-1} - \Psi_h \quad (12)$$

and

$$u_* = ku[[\ln(\frac{z-d_0}{Z_{0m}}) - \Psi_m]^{-1} \quad (13)$$

where *k* is the Von-Karman constant , u_* the friction velocity, *z* reference height, d_0 zero-plane displacement height, Z_{0m} the effective aerodynamic roughness, Ψ_m and Ψ_h the stability correction functions for momentum and sensible heat transfer respectively. kB^{-1} is excess resistance to heat transfer (Chamberlain,1968) and can be derived from the model proposed by Su et al.(2001).

To model sensible heat flux on a large scale using remote sensing data, the similarity formulation based on the Monin-Obukhov similarity (MOS) theory has been the most widely used approach (Brutsaert,1982,1999; Su,et al.,2000). This approach has been proved to be successful to calculate regional average surface sensible heat fluxes (Lhomme et al.,1994; Bastiaassen,1995; Wang et al., 1995; Ma et al., 1997,1999; Su et al., 2000). Based on this approach, combining Eqs 11, 12 and 13, the regional sensible heat flux *H* can be derived from the following equation:

$$H = \frac{\rho C_p k^2 u_B \left(T_{sfc} - T_{air-B}\right)}{[\ln \frac{z_B - d_0}{Z_{0m}} + kB^{-1} - \Psi_h][\ln \frac{z_B - d_0}{Z_{0m}} - \Psi_m]} \tag{14}$$

where Z_B is the bulk atmosphere boundary layer (ABL) height, u_B and T_{air-B} are wind speed and air temperature at the ABL height respectively. In this study, these variables over the Longxi Loess plateau area are determined with the aid of field measurements. Z_{0m} is the effective aerodynamic roughness length derived by relating the effective stress to the surface characteristics (Wieringa,1992; Ma et al.,2002).

2.1.4 The Latent Heat flux λE

The latent heat flux between surface and atmosphere can be expressed as:

$$\lambda E = \frac{\rho C_p \left(q_s - q_a\right)}{\gamma . r_a} \tag{15}$$

Residual approach based on surface energy balance Eq. (1) is widely used to calculate surface latent heat flux. Specifically, after computing the sensible heat flux (H) with Eq.(14), the net radiation (R_n) with Eq.(2) and soil heat flux (G_0) with Eq.(9), the latent heat flux can be derived as the residual of the energy budget theorem from Eq (1) as

$$\lambda E = R_n - G_0 - H \tag{16}$$

2.2 Calculation of instantaneous evaporative fraction

Based the surface energy balance system model (SEBS) discussed above, the evaporative fraction Λ using NOAA/AVHRR data of Oct.1st, 2002 (6:26AM) can be given below after the net radiation R_n, sensible heat flux H, latent heat λE and soil heat flux G_0 are derived:

$$\Lambda = \frac{\lambda E}{R_n - G_0} = \frac{\lambda E}{\lambda E + H} \tag{17}$$

where *H = 0,* $\Lambda = 1$ (water surface) , λE = 0 , $\Lambda = 0$ (dry land surface).

The calculated evaporative fraction is shown in Fig.2. Higher values (0.6-0.9) occur in the Liupan Mountains, Qinling Mountains, Tibet Plateau, Qilianshan Mountains and several reservoirs where more water is available for evaporation. A large area of low evaporative fraction, ranging between 0 and 0.25 (dark areas in Fig. 2), is found in Yellow River Valley, Zhuli River basin and the northern desert area, suggesting that a major portion of the study area is characterized by lack of water for evaporation.

2.3 Calculation of daily evaporation

The above-calculated evaporative fraction Λ is instantaneous value (6:26AM) and it can be extrapolated to daily Λ :

$$E_{day} = \frac{8.64 \times 10^7 \Lambda_{day} \times (R_{nd} - G_{0d})}{\lambda \cdot \rho_w} \tag{18}$$

where E_{day} is the actual daily evaporation (mm d^{-1}). Λ_{day} the daily evaporative fraction, Λ_{inst} (instantaneous evaporative fraction) has a constant relationship with the daily Λ_{day} . R_{nd} and G_{0d} are the daily net radiation flux and soil heat flux respectively, ρ_w the density of water (Kgm^{-3}) $\rho_w = 1000 kg/m^3$, λ the latent heat of vaporization (JKg^{-1}) and can be calculated as :

$$\lambda = [2.501 - 0.00237 * T_a)] \times 10^6 \tag{19}$$

where T_a is mean air temperature (^0C). The daily soil heat flux G_{0d} should be close to zero because of the fact that daytime downward flux is approximately equal to the nighttime upward flux. The daily ET thus depends on the daily net radiation flux as following:

$$E_{day} = \frac{8.64 \times 10^7 \Lambda_{day} \times R_{nd}}{\lambda \cdot \rho_w} \tag{20}$$

$$R_{nd} = (1 - r) K_{24}^{\downarrow} + L_{24} \tag{21}$$

where $K_{24}^{\downarrow}$ is daily incoming global radiation and L_{24} is daily net long wave radiation.

The calculated daily ET generally matches the instantaneous evaporative fraction in Fig.2. Low ET ranging between 0 and 1.0 mm/d (black areas in Fig.3) is found in the Zuli basin, Yellow River valley and northern desert. The ET in the Qilian Mountains, Tibet Plateau, Liupan Mountains and Qinling Mountains are evidently higher than in those low-elevation valleys and basins and also increases with increasing elevation in these high-elevation mountains and plateau (Fig.3). This spatial distribution patterns suggest that both increased precipitation and better vegetation coverage in the mountains contribute to the elevated ET.

3. DATA PROCESSING

In order to use SEBS model to calculate evapotranspiration, several land surface biophysical parameters, such as albedo, land surface temperature, emissivity, and NDVI, have to be determined from remote sensing data (NOAA/AVHRR). The calculation of both the surface bi-directional reflectance and vegetation index (NDVI) are based on AVHRR channels 1 and 2 (Valiente et al., 1995). The algorithm for deriving surface temperature is based on a theoretical split-window algorithm of Coll and Caselles (1997). Emissivity is calculated using the

vegetation cover method of Valor and Caselles (1995). Albedo, land surface temperature, emissivity, and vegetation index (NDVI), in conjunction with land surface *in-situ* observed data and atmospheric PBL data, are applied within the surface energy balance system model (SEBS) to calculate the actual evapotranspiration. The needed PBL (Planetary Boundary Layer) data for calculating sensible heat flux (see Section 2.1.3) include PBL height (m), PBL wind speed (m/s), PBL relative humidity, PBL potential air temperature (K), PBL air pressure (Pa) and surface air pressure (Pa) and were obtained by tether balloon sounding or radiosonde.

4. VERIFICATION

In order to check whether the SEBS model is acceptable for estimating daily actual evapotranspiration or not, we compared ground station-measured evaporation with SEBS mode-estimated evaporation for non-vegetative (i.e., no transpiration) land surface. Two places, Yongjing weather station near Liujiaxia reservoir and Qianyang weather station near Fengjiashan reservoir, are selected for ET verification.

Liujiaxia Reservoir, about 5 km away from Yongjing weather station, covers an area of 130 km^2. Hongjiashan reservoir, 3 km away from Qianyang station covers an area of 10 km^2. According to the observational data from these two weather stations, conversion factor of evaporation from 0.2-m diameter pan to 5-m diameter pan is 0.469. We assume that the 5-m diameter evaporation pan reasonably represents the reservoir evaporation condition. That is

$$E_R = E_5 = 0.469 * E_{0.2} \tag{22}$$

where E_R is reservoir actual ET, E_5 ET of 5-m pan, $E_{0.2}$ ET of 0.2-m pan. The data from the tow stations are available for the entire year of 2002 and one day per month for the year (totally 12 days from 12 months corresponding the remote sensing data dates) was selected for the purpose of ET verification. Table 1 shows that the absolute errors between the estimated values and observation values of these two places are relatively small, varying from –0.43 to 0.88. The relative errors are mostly less than 20%.

Table 1, Figs.4 and 5 demonstrate that the SEBS model-estimated values for the Liujiaxia and Fengjiashan Reservoira are in reasonably good agreement with the station-measured values at the nearby weather stations, suggesting that the remote sensing-aided SEBS modeling can achieve an acceptable level of accuracy in estimating actual evapotranspiration in semiarid regions.

5. CONCLUSIONS AND DISCUSSIONS

Our experimental study to estimate ET in the Western Chinese Loess Plateau shows that an acceptable estimation of ET in semi-arid area can be achieved at regional scales by using NOAA/AVHRR data-derived parameters as the input variables in simulating the surface energy balance. The spatial distribution of the estimated ET shows that ET is the highest in the well-vegetated high elevations and major water bodies (white and pink areas in Fig 3), intermediate in hilly plateau areas (green and blue areas in Fig. 3), and the lowest in low-elevation valleys and basins and also in northern desert areas (black areas in Fig. 3). The regional-scale distribution shows that ET in the western Chinese Loess Plateau is primarily determined by vegetation coverage, which is in turn determined by soil water availability. This study suggests that the spatial distribution in ET is primary modulated by the temperature difference and humidity difference between land surface and nearly surface atmosphere. The results show that in the areas where soil moisture is higher and vegetation coverage is better, the energy transfer between land surface and nearly surface atmosphere is accomplished through latent heat flux, while in the lowlands where soil moisture is lower and vegetation coverage is poorer, the energy transfer is primary through sensible heat flux.

ACKNOWLEDGEMENT

This research is financially supported by a grant from “The Project of Retrieving Remote Sensing Key Land Parameters” of “Hi-tech Research and development program of China, 863 program”(Grant No.:2001AA135110) and "Key Teacher Program" of the Chinese Education Ministry to Feng Zhaodong (Lanzhou University, 2000) on his project: "Watershed Hydrology and Landscape Ecology in the Gansu Loess Plateau: GIS and RS-assisted Modeling Approach"(Grand No.:ETD-2000-65)

REFERENCES

1. Albert Rango and Ahlam I. Shalaby, 1998a, Operational applications of remote sensing in Hydrology :success, prospects and peoblems, *Hydrological Sciences*, 43(6):947-969

2. Bastiassnssen, W.G.M.,. Pelgrum, H., Wang, J., Ma, Y., Moreno, J.F., Roerink, G.J., and Van der Wal, 1998a, A remote sensing surface energy balance algorithm for land (SEBAL) 2. Validation, *Journal of Hydrology* 213:213-229

3. Becker,F. & Z-L.Li , 1990a, Surface temperature and Emissivity at various scales: definition,measurements and related problems, *Remote Sens. Rev.* 12:.225-253

4. Bob Z. Su, 2000, Remote sensing of land use and vegetation for mesoscale hydrological studies, *Int. J. Remote Sensing,* 21:213-233

5. Bob Z. Su, A surface Energy Balance System (SEBS) for estimation of turbulent heat fluxes from point to continental scale. In Bob Z. Su and C. Jacobs (eds.), 2001b, Advanced Earth Observation-Land Surface Climate, Publication of the National Remote Sensing Board, USP-2, 01-01, pp 183

6. Boni, G., Entekhabi, D., and Castelli, F, 2001a, Land Data Assimilation with Satellite Measurements for the Estimation of Surface Energy Balance Components and Surface Control on Evaporation¡, *Water Resour. Res.* 37: 1713-1722

7. Coll, C. and V. Caselles, 1997 b, A split-window algorithm for land surface temperature from AVHRR data, *validation and algorithm comparison*,JGR,

8. Francesca Caparrini, Fabio Castelli and Dara Entekhabi, 2003a, Mapping of Land-Atmosphere Heat Fluxes and Surface Parameters with Remote Sensing Data , *applied meteorology*, 07(3):605-633

9. Gutman, G., and Ignatov, V., 1998a, The derivation of the green vegetation fraction from NOAA/AVHRR data for use in numerical weather prediction models, *International Journal of remote sensing*, 19(8):1533- 1543

10. Jerald A. Brotzge and Kenneth C. Crawford, 2000a, Estimating sensing heat flux from the Oklahoma mesonet, *Journal of Applied Meteorology*, 39: 102-116.

11. Ma Yaoming and Osamu Tsukamoto, 2002b Combining satellite remote sensing with field observations for land surface heat fluxes over inhomogeneous landscape, China Meteorological Press.

12. Toby, N.C., 1991a, Modeling stomatal resistance: an overview of the 1989 workshop at the Pennsylvania State University, *Agricultural and Forest Meteorology* 54:103-106

13. Valiente,J.A, Nunez,M., Lopez-Baeza,E. and Mereno, J.F. 1995a, Narrow- band to broad-band conversion for Meteosat-visible channel and broad- band albedo using both AVHRR-1 and –2 channels, *Int. J. Remote Sens*. 16:1147-1166

14. W.G.M. Bastiaanssen, 2000a, SEBAL-based sensible and latent heat fluxes in the irrigated Gediz Basin, Turkey, *Journal of Hydrology*, 229:.87-100.

15. Vanzanten, M. C, 2002a ,Radiative and Evaporative Cooling in the Entrainment Zone of Stratocumulus – the Role of Longwave Radiative Cooling Above Cloud Top.; *Boundary-Layer Meteorology*, 102(2): 253-280

16. Win C. de Rooy and A.A.M. 1999a, Holtslag, Estimation of surface radiation and energy flux densities from single-level weather data, *Journal of Applied Meteorology*, 38:526-540

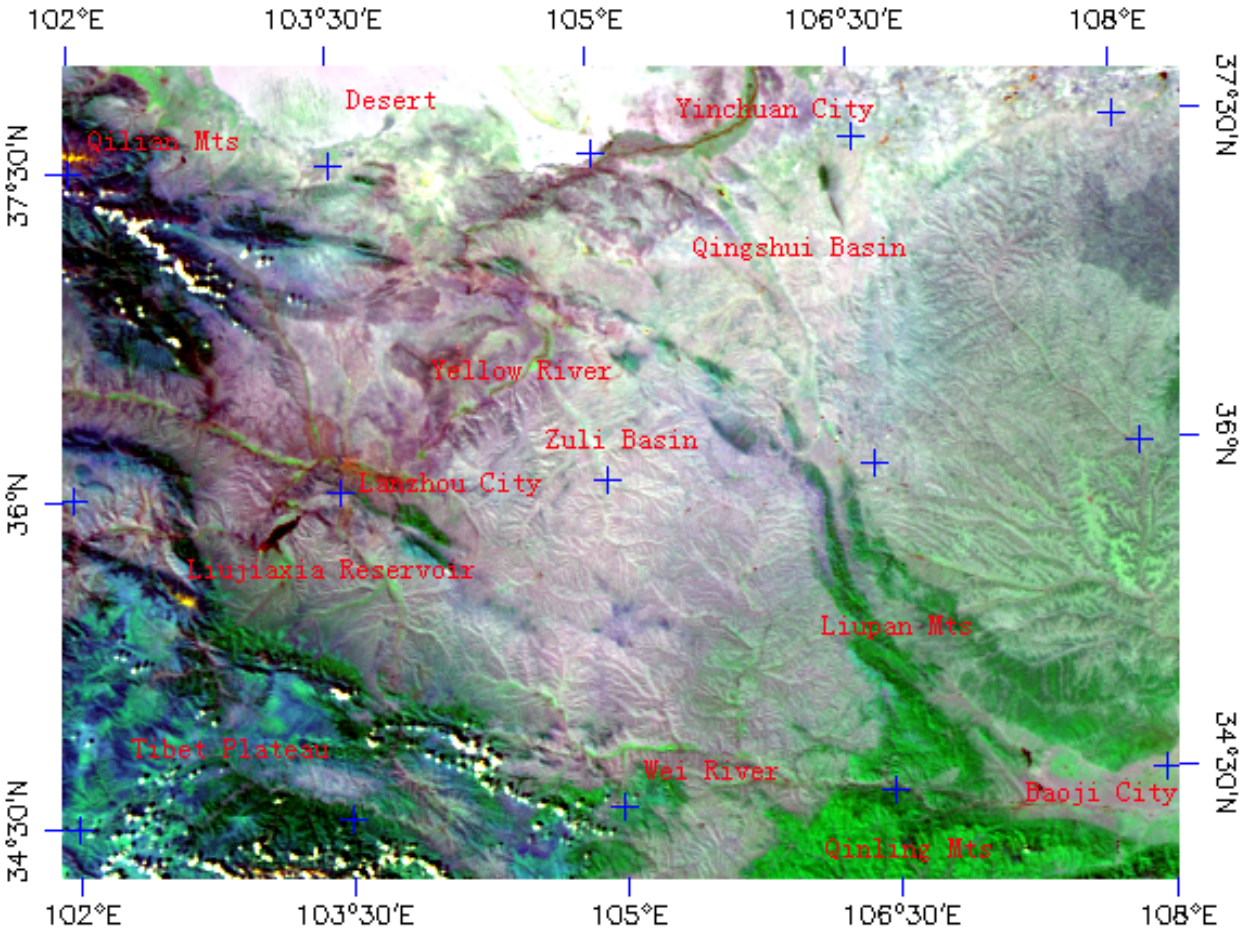

Fig.1. The western Chinese Loess Plateau based on NOAA/AVHRR (6:26 Am, Oct. 2, 2002)

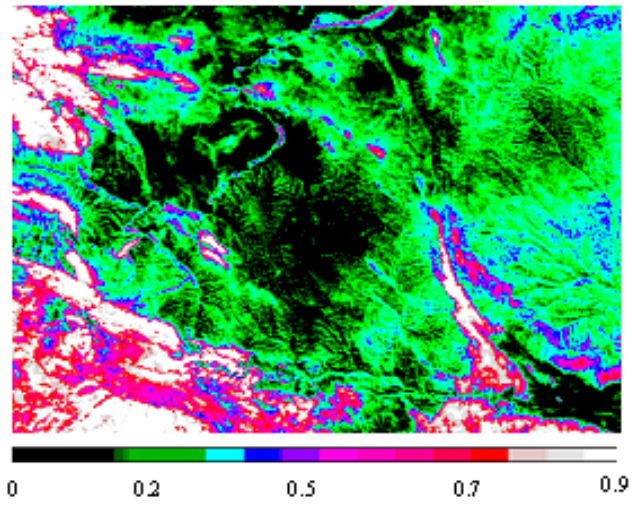

Fig.2. Regional distribution of evaporative fraction over the Western Chinese Loess Plateau derived from NOAA/AVHRR data on Oct. 2nd 2002 (6:26AM)

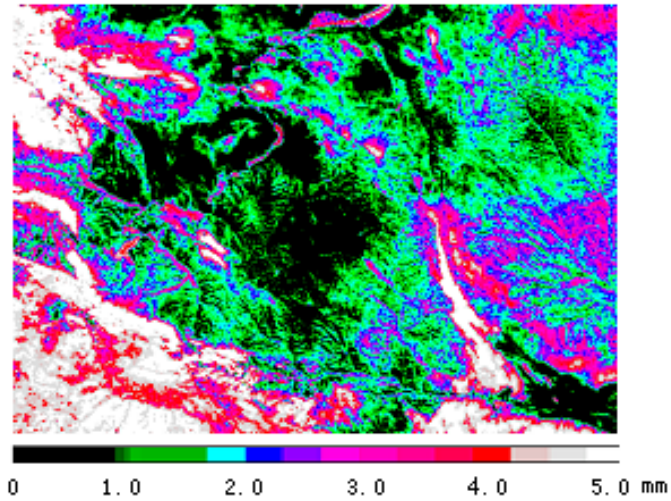

Fig.3. Regional distribution of daily ET over the Western Chinese Loess Plateau derived from NOAA/AVHRR data on Oct. 2nd 2002 (6:26 AM)

Table 1. Comparison between observed and estimated daily ET

Sites	Items	Jan.6th	Feb.12th	Mar.7th	Apr.20th	May.27th	Jun.24th	Jul.12th	Aug.27th	Sep.27th	Oct.1st	Nov.8th	Dec.12th
Liujiaxia reservoir	Estimated value	0.7	1.27	1.92	4.69	2.77	4.5	5.21	4.41	2.63	2.59	1.03	0.47
	Observed value	0.56	0.86	2.34	3.86	3.14	5.12	5.86	5.36	2.05	2.36	1.26	0.24
	Absolute error	0.14	0.41	-0.42	0.83	-0.37	-0.62	-0.65	-0.95	0.58	0.23	-0.23	0.23
	Relative error (%)	20	32	22	18	13	14	12	22	22	9	22	49
Fengjia shan reservoir	Estiamted value	0.89	1.64	2.06	3.14	3.56	3.42	5.25	2.81	2.44	2.32	1.22	0.23
	Observed value	0.74	1.58	1.89	2.66	2.78	3.1	4.68	3.2	3.32	2.37	1.65	0.34
	Absolute error	0.15	0.06	0.17	0.48	0.64	0.46	0.57	-0.39	0.88	-0.05	-0.43	-0.11
	Relative error (%)	17	4	8	15	19	13	11	14	36	2	35	47

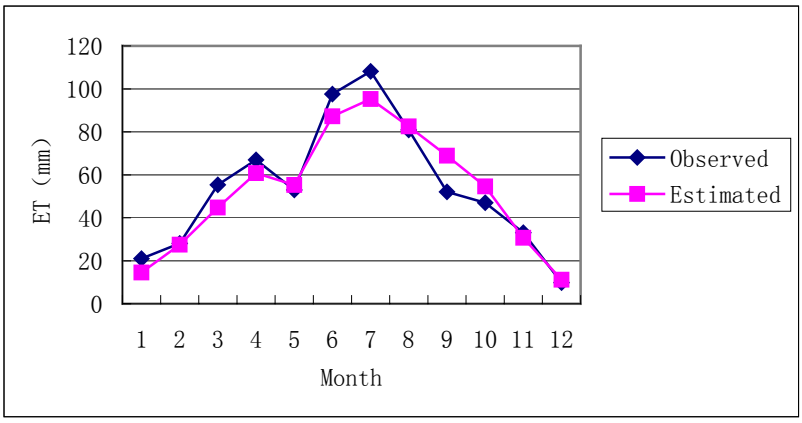

Fig. 4 Daily ET comparison between observed values and estimated values at Liujiaxia Reservoir

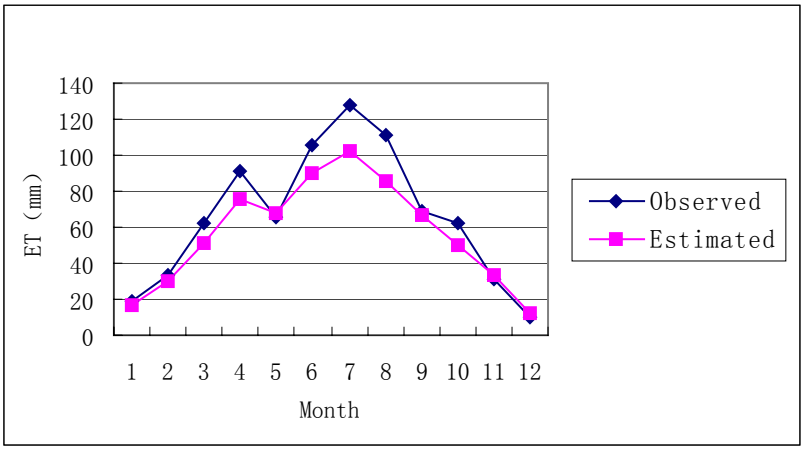

Fig..5. Daily ET comparison between observed values and estimated values at Fengjiashan Reservoir